Conformation of Neutral Polyampholyte Chains in Salt Solutions: A Light Scattering Study

M. Skouri,[†,‡] J. P. Munch,[†] S. J. Candau,[†] S. Neyret,[§] and F. Candau*[,§]

Laboratoire d'Ultrasons et de Dynamique des Fluides Complexes, Unité de Recherche Associée au CNRS No. 851, Université Louis Pasteur, 4 rue Blaise Pascal, 67070 Strasbourg Cedex, France, and Institut Charles Sadron (CRM—EAHP), 6 rue Boussingault, 67083 Strasbourg Cedex, France

Received July 8, 1993; Revised Manuscript Received October 13, 1993[•]

ABSTRACT: The salt aqueous solution properties of a low charge density polyampholyte terpolymer with a balanced stoichiometry of charges were investigated by static and dynamic light scattering. At high ionic strength, the sample is entirely soluble and the chains exhibit an excluded volume conformation. When the salt content is lowered, part of the sample precipitates, leaving in the supernatant highly swollen chains. The results are interpreted by assuming that, due to different reactivity ratios of the monomers, there is a distribution of the net charges among the polymer chains. By varying the salt content, one performs a fractionation of the polyampholyte chains according to their net charge.

Introduction

Polyampholytes, which are copolymers containing both positive and negative charges distributed along the chain present great potential for applications due to their interesting aqueous solution properties.[1-14] The introduction of ionic groups of opposite signs onto the polymer chain results in a complex solution behavior which is essentially controlled by electrostatic interactions. For example, a polyampholyte with a balanced stoichiometry (same number of negative as positive monomers) is usually insoluble in water but becomes soluble upon addition of salt, which screens the interactions and weakens the attractions.[1] This results in an antipolyelectrolyte behavior, with enhanced viscosity upon increasing the ionic strength, making these polymers well adapted to high-salinity media.

While a large number of theoretical work exists on the structure of polyelectrolytes, much less attention was paid to polyampholytes[15] until recently when different groups studied by theoretical means and by simulation the behavior of such polymers.[16-20] However, opposite conclusions were reached on whether the conformation in pure water of a neutral polyampholyte is stretched or compact. Both Monte-Carlo simulations and analytical arguments predict in fact that the conformation is very sensitive to the charge distribution. Polyampholytes with an overall constraint of charge neutrality are found to collapse into compact globules.[16] If however, there is a random distribution of the oppositively charged monomers, it was argued that the polymer chains can be stretched due to the occurrence of a small net charge.[17] Copolymers with an average net charge have also been studied theoretically by Higgs and Joanny.[16] It was shown that depending on the salt content, the solution behavior is dominated by either the attractive polyampholyte effect or by the repulsive electrostatic effect.

In a recent series of papers, Corpart and Candau described the synthesis,[21] the characterization,[22] and the aqueous solution properties[23] of a series of high charge-density polyampholytes formed of sodium 2-(acrylamido)-2-methylpropanesulfonate (NaAMPS) and [2-(methacryloyloxy)ethyl]trimethylammonium chloride (MADQUAT). The preparation of polyampholytes by means of a microemulsion polymerization technique was shown to present several advantages over other conventional processes. In particular, the process allows the production of very high molecular weight polymers (up to 1.7×10^7) at rapid reaction rates. Another characteristic is related to the microstructure of these polyampholytes. Microemulsion polymerization yields copolymers more homogeneous in composition, with a microstructure not far from random (reactivity ratios $r_1 r_2 = 1.6$), while polymerization in solution usually leads to copolymers with a strong tendency to alternation.[11,12,22] This result was attributed to differences in mechanism and microenvironment between the two processes.[22]

Experimental results obtained by turbidimetry and viscometry on polyampholytes either neutral or with a large net charge[23] were found to be in qualitative agreement with the model of Higgs and Joanny.[16]

The present paper reports the study of a low charge density terpolymer with a balanced stoichiometry of charges. The sample was prepared using a microemulsion polymerization and by incorporating acrylamide (AM) as a neutral water-soluble monomer along with NaAMPS and MADQUAT as the charged monomers. We analyze here the influence of added salt on the solubility of the terpolymer as well as on the conformational behavior in the dilute regime.

Experimental Section

Materials. [2-(Methacryloyloxy)ethyl]trimethylammonium chloride (MADQUAT) was supplied by Elf-Atochem as a 75% wt/wt aqueous solution. 2-(Acrylamido)-2-methylpropanesulfonic acid (AMPS), obtained from Cassella, was recrystallized from dry methanol prior to use. Neutralization at pH $\simeq$ 9 was achieved by slow addition of AMPS to an aqueous sodium hydroxide solution. Acrylamide (AM) from Aldrich was recrystallized twice from chloroform and the hydrophobic initiator AIBN (2,2'-azobis[isobutyronitrile]) was recrystallized twice from ethanol and dried under vacuum. Water was double distilled. The oil is a narrow-cut isoparaffinic mixture, Isopar M from Esso Chemic, which was filtered before use (boiling range: 207–275 °C). The surfactant is a blend of sorbitan sesquioleate (Arlacel 83, HLB: hydrophile–lipophile balance = 3.7) and a poly(oxyethylene)

* To whom correspondence should be sent.
† Université Louis Pasteur.
‡ Permanent address: Université Cadi Ayyad, Faculté des Sciences Semlalia, Laboratoire d'Electronique et d'Instrumentation, Boulevard du Prince Moulay Abdellah, B.P. S15, Marrakech, Maroc.
§ Institut Charles Sadron.
• Abstract published in *Advance ACS Abstracts*, December 1, 1993.

0024-9297/94/2227-0069$04.50/0

sorbitol monooleate with 40 ethylene oxide residues (G 1086, HLB = 10.2), supplied by ICI speciality Chemicals.

The transparent and thermodynamically stable microemulsions were prepared (wt/wt) with stirring by adding the aqueous solution of monomers (adjusted to pH $\simeq$ 7) to the mixture of surfactants, AIBN, and Isopar M. The recipe used was the following (w/w): Isopar M, 44%; monomers, 22%; water, 22%; nonionic emulsifiers, 12%.

Polymerization Procedure. The polymerization experiments were carried out in water-jacketed reaction vessels, after bubbling purified nitrogen through the microemulsion to eliminate oxygen. The monomer feed was initiated with AIBN as the oil-soluble initiator (0.3 wt % based on monomers) by irradiation at 20 °C from a source of ultraviolet light (mercury lamp, Philips).

Total conversion to copolymer was achieved within <30 min. The product of the polymerization was a clear and stable microlatex. After polymerization, the latex was poured into an excess of 2-propanol, and the precipitated copolymer was separated and washed several times. It was then filtered out and dried under vacuum at 45 °C. To eliminate impurities (monomers, residual salt, emulsifiers, etc.), the resulting polymer powder was subsequently dissolved in 0.5 M NaCl aqueous solutions and dialyzed against deionized water before recovering by freeze-drying.

Copolymer Composition. A monomer feed containing NaAMPS/AM/MADQUAT in a molar ratio 3.77/92.48/3.75 was polymerized in a microemulsion according to the recipe given above and polymerized up to complete conversion. The terpolymer composition was determined by elemental analysis. The weight percentage of C, H, and N was determined with a Carbo Erba elemental analyzer, the sodium content by atomic adsorption spectrophotometry, and Cl, N, and S by mineralization using the Schöninger method. The water content in the copolymer was measured by Karl Fisher's method with an automatic KFE 452 titrimeter. The elemental analysis data after correction for water content were found to be NaAMPS, 3.83; AM, 92.18; and MADQUAT, 3.99, in excellent agreement with the initial monomer feed.

As for other high charge-density polyampholytes,[22] a more complete analysis of the data shows that the sample after dialysis tends to self-neutralize almost completely; i.e. the anionic and cationic monomers are completely paired with no residual sodium or chloride counterions left in the solution.

Light Scattering. As polyampholyte solutions are very sensitive to shear degradation and to aggregation, the polymer stock solutions were made by dissolving the polymer at a concentration of $\simeq 5 \times 10^{-3}$ g cm^{-3} in 0.5 or 0.2 M NaCl aqueous solution 48 h before the measurements under gentle stirring. The solutions were subsequently diluted to appropriate concentrations (down to 2×10^{-5} g cm^{-3}) at the prerequisite salt concentration and were made dust-free by centrifugation.

The samples are hygroscopic, and for all experiments, the concentrations were corrected for water content.

The optical source on the light scattering apparatus is a Spectra-Physics argon ion laser operating at $\lambda_0 = 4880$ Å. The scattered intensity and the time-dependent intensity correlation function are obtained by using a 256-channel digital correlator (ALV 8000). The scattering angle could be varied between 15 and 145°. The scattered intensities reported on the different figures of this paper have been normalized by the intensity scattered by the toluene.

The intensity data were processed by using the method of cumulants[24] to obtain the average decay rate $\langle\Gamma\rangle$ of the field autocorrelation function and the variance $v = (\langle\Gamma^2\rangle - \langle\Gamma\rangle^2)/\langle\Gamma\rangle^2$. For most systems investigated in this study, we observe a moderate distribution of exponential decays $0.1 \leq v \leq 0.25$. Only the more concentrated samples exhibit a correlation function with two distinct decay rates.

All the experiments were performed at $T = 20$ °C. The refractive index increments dn/dc were determined on dilute samples in NaCl aqueous solutions (2×10^{-3} g cm$^{-3} < C < 10^{-2}$ g cm^{-3}) with a Brice-Phoenix differential refractometer (wavelength $\lambda = 632.8$ nm). The dn/dc were found to be 0.170 and 0.175 cm^3 g^{-1} in 1 and 0.5 M NaCl aqueous solutions, respectively. The values of dn/dc at lower salt contents were obtained by extrapolation, using the two above values.

The viscosity values of the solvents were taken as tabulated in the handbooks and are as follows

[NaCl](M)	5×10^{-3}	10^{-2}	5×10^{-2}	0.1	0.2	0.5
η_0 (mPa s)	1.00	1.002	1.006	1.011	1.021	1.048

Experimental Results

(a) Sample Characterization. To determine the morphological characteristics of the samples, the polymer is dissolved in 0.2 and 0.5 M NaCl brines. With such salt contents, and for the polymer concentrations used, the sample is entirely solubilized. The electrostatic interactions are screened out since the Debye–Hückel length κ^{-1} is equal to 6.8 and 4.3 Å, respectively.

Angular Distributions of the Scattered Intensity. The properties of the light scattered by polymer solutions depend on the concentration range and on the relative magnitude of a characteristic length scale explored in the light scattering experiment. In dilute solutions, the characteristic length is the radius of gyration R_G. In semidilute solutions, above a concentration C^* when the polymer chains begin to overlap, the characteristic length is the correlation length ξ that decreases upon increasing concentration.

In the Guinier regime, i.e. if qR_G or $q\xi \ll 1$, the angular distribution of the excess of scattered intensity with respect to the solvent has well-known forms, namely

$$C/I = (C/I(0))\left(1 + \frac{q^2R_g^2}{3} + ...\right) \quad (1)$$

or

$$C/I = (C/I(0))(1 + q^2\xi^2) \quad (2)$$

with

$$\lim C\to 0 \left(\frac{C}{I(0)}\right) = A\left(\frac{dn}{dC}\right)^{-2}\frac{1}{M_w} \quad (3)$$

where A is an apparatus constant that is determined by using toluene as a reference sample. M_w is the weight average molecular weight of the polymer.

If qR_G (or $q\xi$) $\gg 1$, light sees essentially the interior of the flexible polymers, the conformation of which depends on the quality of the solvent. The corresponding scattering pattern is known to be a power law of q, $I(q) \sim q^{-d}$ with $d = 1$ for a stretched polymer, $d = {}^5/_3$ for an excluded volume regime, and $d = 2$ for a Gaussian chain.[25]

If the data are obtained in a range around $qR_G = 1$, one can use the Fisher–Burford expression[26] that has been applied to studies on fractal colloidal aggregates[27] and on wormlike micelles[28] and that has the asymptotic behavior for high and low q's corresponding to the behavior described above:

$$I(q) = I(0)\frac{1}{\left[1 + \frac{2}{3d}q^2R_g^2\right]^{d/2}} \quad (4)$$

Figure 1 shows the log–log variation of I/C versus q^2 for systems with different polymer concentrations and dissolved in 0.5 and 0.2 M NaCl aqueous solutions, respectively. One observes clearly a crossover from a Guinier behavior in the low q range to an intermediate regime characterized by a power law. In the dilute regime the different scattering curves tend to coincide. Upon increasing polymer concentration, they still obey the same

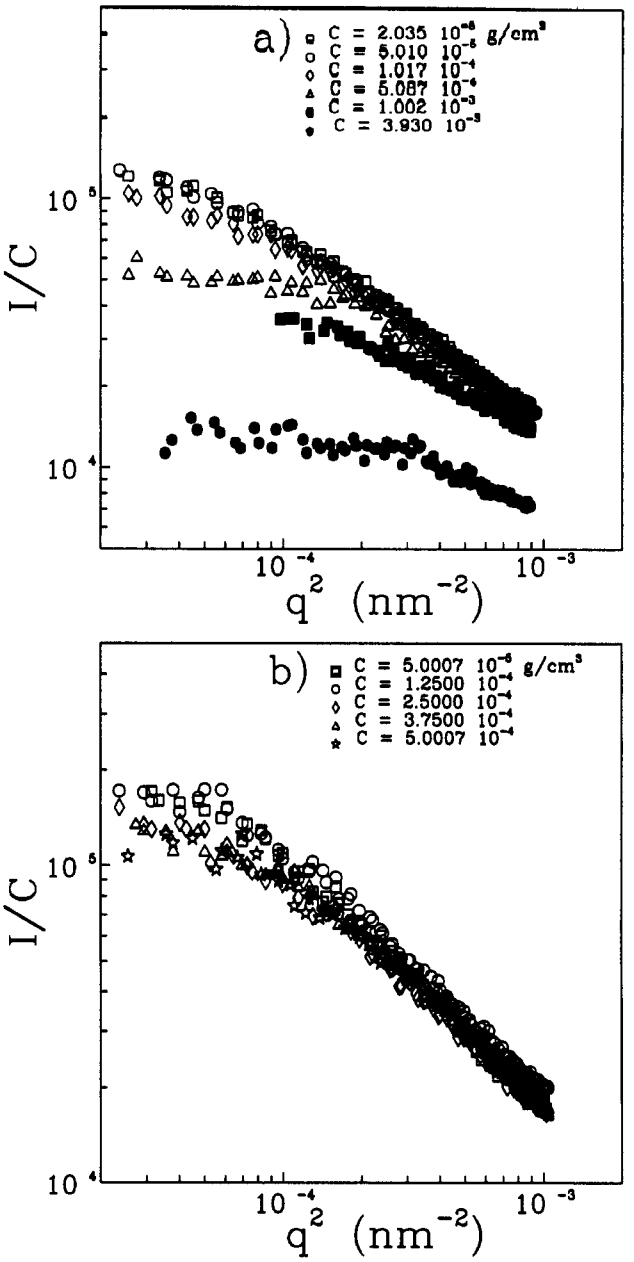

Figure 1. Scattering curves for different polymer concentrations: (a) C_s = 0.5 M; (b) C_s = 0.2 M.

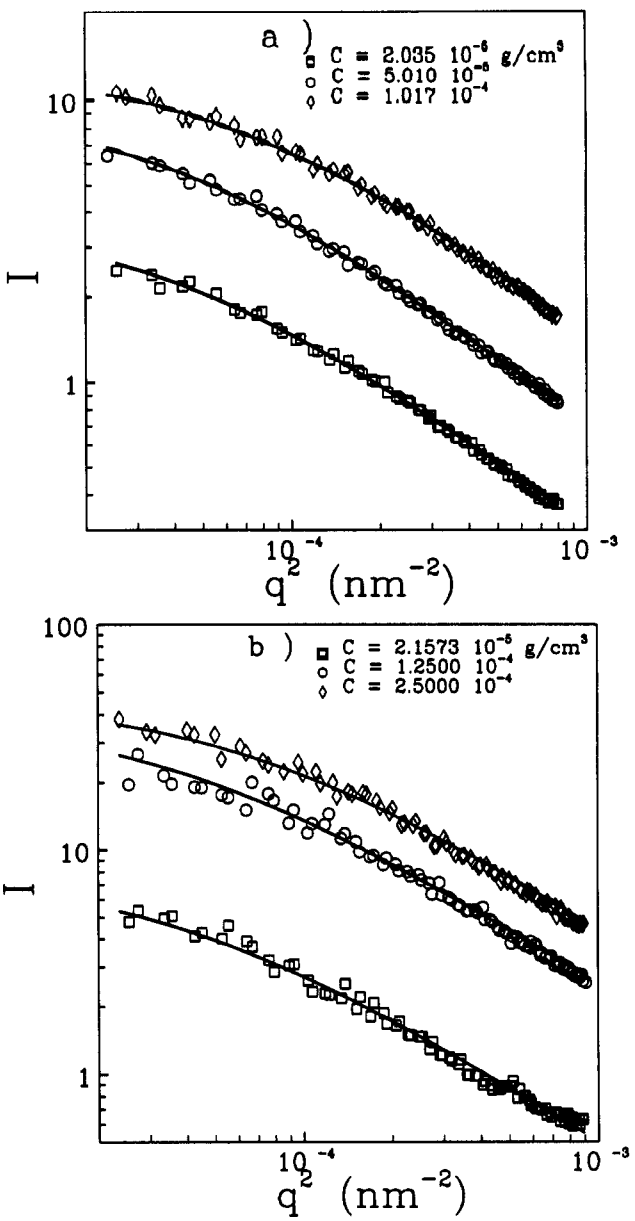

Figure 2. Angular distributions of scattered light for different polymer concentrations: (a) C_s = 0.5 M; (b) C_s = 0.2 M. The lines are the fits to the experimental data of the Fisher–Burford expression (see text).

behavior in the high q range, but the crossover wavevector q^* between the Guinier regime and the intermediate regime is shifted to higher q values. This could be interpreted as the onset of the semidilute behavior for which the crossover occurs at $q^*\xi = 1$ instead of $q^*R_G = 1$ in the dilute regime with $\xi \leq R_G$. From the data of Figure 1 one can estimate 10^{-4} g cm^{-3} < C^* < 5×10^{-4} g cm^{-3}. The concentration dependence of the scattered intensity in the $q \to 0$ limit does not confirm this result. As a matter of fact, this intensity increases steadily with the polymer concentration whereas one would expect from the well-known behavior of neutral polymers a maximum of the scattered intensity at the crossover concentration C^* between the dilute and the semidilute regimes. In this respect, one must point out that for polymer concentrations $C \geq 10^{-3}$ M one clearly observes in the autocorrelation function obtained in dynamic light scattering a slow mode. This could be an indication of the formation of aggregates that would form above C^* and would contribute significantly to the scattering. We will come back later to this point.

In the dilute range one can use in principle the classical representation C/I versus q^2 to obtain the radius of gyration R_G and the molecular weight M_w according to eqs 1–3. However, as most of the data lie in the crossover region between the Guinier and the intermediate regime, it is preferable to use the Fisher–Burford expression (cf. eq 4). Figure 2 shows the fits of such an expression to the scattering curves obtained for samples with different polymer concentrations and salt contents 0.2 and 0.5 M, respectively. From the fits we obtain for a given polymer concentration the fractal exponent d and an apparent radius of gyration. The values of the apparent radius of gyration were found to be in good agreement with the initial slope of the curve $C/I = f(q^2)$. The extrapolation to zero polymer concentration of the apparent radius of gyration leads to the following estimates of R_G

$$R_G = (2400 \pm 200)\ \text{Å in 0.5 M NaCl solution}$$

$$R_G = (2500 \pm 200)\ \text{Å in 0.2 M NaCl solution}$$

As for d, we obtain

$$d = 1.6 \pm 0.1 \text{ in both 0.5 and 0.2 M NaCl solutions}$$

The above values are characteristic of an excluded volume

regime. They are slightly larger than those obtained from the slopes of the straight lines measured in the high q limit of the log–log plots of $I(q)$ (cf. Figure 1). This could be due to a polydispersity effect that smoothes the crossover between Guinier and intermediate regimes, thus reducing artificially the variation of $I(q)$. It must also be noted that the highest values of qR_G attainable in our experiments are around 8; it is well-known that data analyzed in an up-limited qR_G range lead to a slightly reduced exponent.

The extrapolation of (C/I) to zero q and zero C provides an estimate of the weight average molecular weight (cf. eq 3).

One obtains

$$M_w = (9.1 \pm 1) \times 10^6 \text{ in 0.5 M NaCl solution}$$

$$M_w = (9.5 \pm 1) \times 10^6 \text{ in 0.2 M NaCl solution}$$

Dynamic Light Scattering. The dynamic scattering experiments provide also different information, depending on the qR_G range investigated.

In the dilute regime and in the range $qR_G \ll 1$, the autocorrelation function is close to a single exponential with a mean decay rate $\langle\Gamma\rangle$ related to the translational diffusion coefficient D by

$$\langle\Gamma\rangle = Dq^2 \tag{5}$$

$$D = k_B T/6\pi\eta_0 R_H \tag{6}$$

with k_B the Boltzmann constant, T the absolute temperature, η_0 the viscosity of the solvent, and R_H the hydrodynamic radius.

In the intermediate regime, the relaxation of the index fluctuations is due to internal modes of the chains. The shape function has been explicitly obtained for an unperturbed Gaussian chain[29] and can be represented in the limit $qR_G \to \infty$ by a stretched exponential with an exponent $-2/3$. In the case of a polymer in a good solvent, the asymptotic shape is not available analytically although it is not expected to deviate appreciably from that in a Θ solvent.[30] Akcasu et al., using the linear response theory,[31,32] and Lee et al., using an ϵ expansion,[33] developed models for the interpretation of dynamic scattering experiments in terms of the first cumulant $\langle\Gamma\rangle$ of the intermediate scattering function. It was found that

$$\langle\Gamma\rangle = A\frac{k_B T}{\eta_0}q^3 \tag{7}$$

The prefactor was found to be dependent on the quality of the diluent. For solutions in a good solvent $A \simeq 0.08$ according to Akcasu and Benmouna whereas $A \simeq 0.045$ in the derivation of Lee et al. The theoretical curves obtained in these two theories for the variation of $\langle\Gamma\rangle$ versus qR_G are given in Figure 3.

Figure 4 shows the results of dynamic light scattering for solutions in 0.2 and 0.5 M brines, plotted using the log–log representation $(2\Gamma)^{-1}q^2$ versus q^2. Again one observes a net crossover at about the same q values as for $I(q)$ (cf. Figure 1). We have also performed a detailed analysis of the shape function in the intermediate regime. The long time behavior ($t > \langle\Gamma\rangle^{-1}/2$) of the autocorrelation function $G^{(2)}(t)$ of the scattered intensity is well described by a stretched exponential function $A_\beta e^{-(t/\tau_0)^\beta}$ with $\tau_0^{-1} = 2\langle\Gamma\rangle$ and $\beta = 0.657$, a value in good agreement with the theoretical one ($^2/_3$). An example of the profile of $G^{(2)}(t)$ is given in Figure 5 where the logarithm of the normalized autocorrelation function $G^{(2)} = (G^{(2)}(t) - 1)/G^{(2)}(0))$ is plotted as a function of $(t/\tau_0)^\beta$. In this representation, over a decrease of $G^{(2)}$ by a factor 100, a linear behavior is observed which clearly shows that the stretched exponential decay is the dominant feature of the time dependence of $G^{(2)}(t)$.

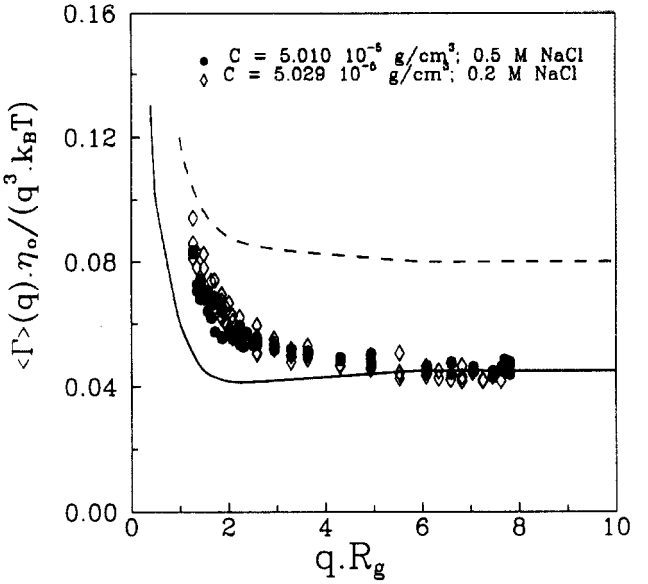

Figure 3. Variations of the reduced first cumulant $\langle\Gamma\rangle(q)\eta_0/k_B T q^3$ as a function of qR_G. The solid curve is the renormalization group calculation of Lee et al.,[32] and the broken curve is that of Benmouna and Akcasu.[31]

In Figure 3 are reported the plots of $\langle\Gamma\rangle\eta_0/k_B T q^3$ versus qR_G for two dilute solutions with salt concentrations respectively equal to 0.2 and 0.5 M. The experimental results are in satisfactory agreement with the theoretical prediction of Lee et al.,[33] mainly in the high q range where the polydispersity plays a lesser role.

The extrapolation of $\langle\Gamma\rangle/q^2$ to zero q leads to the following value for the hydrodynamic radius of the sample

$\langle R_H\rangle = (1500 \pm 100)$ Å in both 0.5 and 0.2 M NaCl solution

The ratio R_G/R_H is found to be $\sim$1.6, that is a value close to the theoretical prediction 1.562 obtained by Oono[34] for a polymer in a good solvent. Again, we have a better agreement with this theory than with the linear response theory that predicts[35] $(R_G/R_H) = 1.86$.

(b) Salt Effect. In the salt and polymer concentration ranges investigated, the solutions appear transparent and the scattering signal is stable at least at the scale of a few days. However, under centrifugation at 2750g, one observes for the samples with NaCl content less than 0.2 M the deposition of a white precipitate, stuck at the bottom of the cell. For a given polymer concentration, the lower the salt content, the larger the amount of precipitate. The intensity scattered from the supernatant solution is smaller than that measured for the sample prior to centrifugation. This suggests the presence in the sample of some aggregates that separate from the solution under centrifugation. The duration of the centrifugation required for the formation of a stable biphasic system is of the order of few hours. A subsequent centrifugation maintains unchanged the intensity scattered by the supernatant. This intensity remains constant in time, thus showing that no redissolution of the precipitate occurs. The precipitate can be easily separated from the supernatant and redissolved in a solution at a higher salt content.

In the present study, we have not attempted to determine the respective amounts of the polymer in the

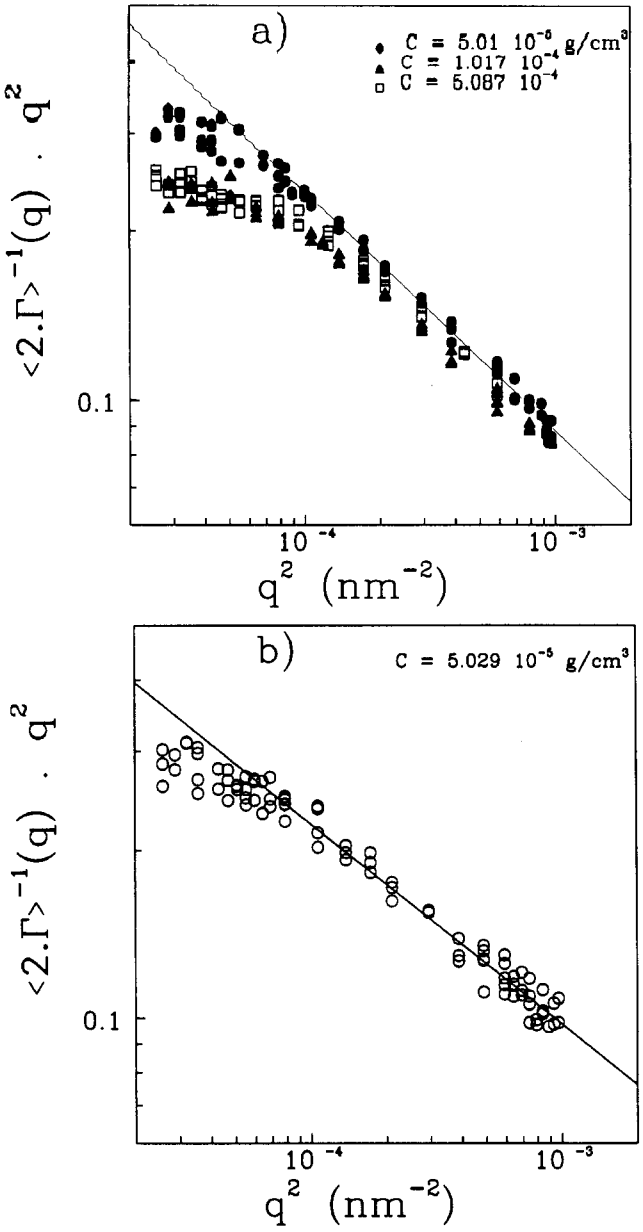

Figure 4. log–log plots of $\langle 2\Gamma\rangle^{-1}q^2$ versus q^2 for different polymer concentrations: (a) $C_s = 0.5$ M; (b) $C_s = 0.2$ M. The straight lines are the best fits to the data in the high q range.

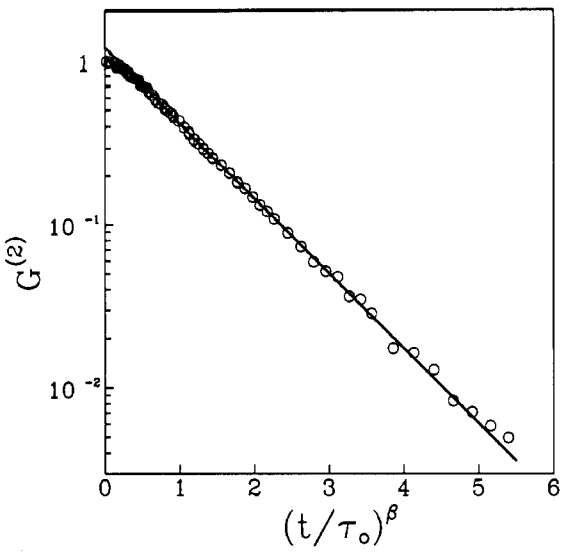

Figure 5. Typical variation of the autocorrelation function of the intensity fluctuations as a function of $(t/\tau_0)^\beta$ with $\beta = 0.657$; $C = 4.35 \times 10^{-5}$ g cm^{-3}, $C_s = 0.2$ M, $\theta = 90°$.

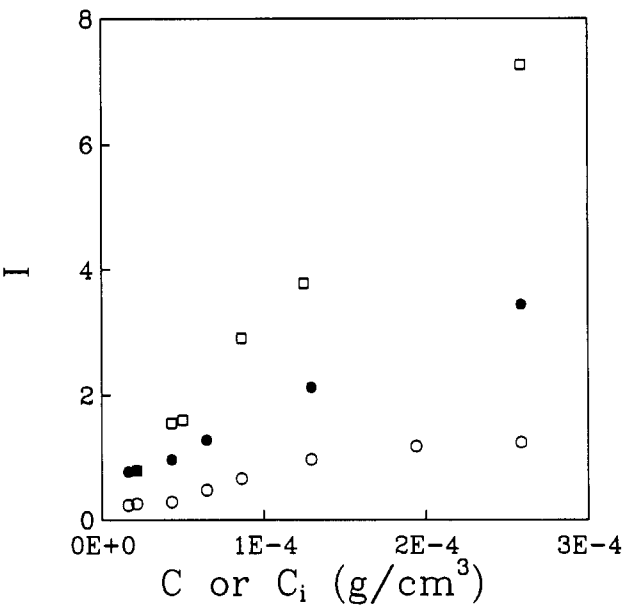

Figure 6. Excess of intensity scattered at $\theta = 90°$ versus concentration C or initial concentration C_i: (□) solutions prepared directly in a 0.2 M NaCl brine; (●) precipitates of solutions prepared at 5×10^{-3} M NaCl, redissolved in a 0.2 M NaCl brine; (○) supernatants of solutions prepared in a 5×10^{-3} M NaCl brine. For the last two systems, the concentration refers to the initial system.

precipitate and the supernatant. However, in order to get an order of magnitude of these amounts for the samples at the lowest salt concentration ([NaCl] = 5×10^{-3}M), we have conducted the following experiment: the precipitates obtained for polymer solutions at different concentrations were redissolved in a brine with 0.2 M NaCl. The intensity scattered from these solutions was found to be significantly larger than those obtained from the supernatants, as shown in Figure 6. Furthermore, the solutions directly prepared in a brine with 0.2 M exhibit even larger scattering. Considering the experimental accuracy that becomes poor for the more dilute samples, and the fact that the three series of systems contain different distributions of polymeric chains, one cannot draw any quantitative conclusions. One can just tell from the results and by assuming in a first approximation that the variations of scattered intensity reflect variations of concentration that at least more than half of the polymer has precipitated. Measurements of the dry content of the precipitate should bring more precise information on that point.

The light scattering results reported in the following refer to either monophasic solutions with a concentration c or to the supernatants relative to the systems with the initial concentration c_i.

The effect of salt on the scattering curves and on the dynamic behavior in the dilute regime, is illustrated in Figures 7 and 8. The most striking feature is that the intermediate regime is extended toward the lower q values as the salt content is decreased. For the system with the smallest salt content, one observes a power law of $I(q)$ in the whole q range experimentally accessible and therefore it is not possible to measure a radius of gyration, nor a molecular weight.

Table 1 summarizes the values obtained for both static and dynamic exponents in the intermediate regime, as a function of salt and polymer concentrations.

Discussion

The solubility behavior of the sample can be qualitatively understood from consideration of the balance between

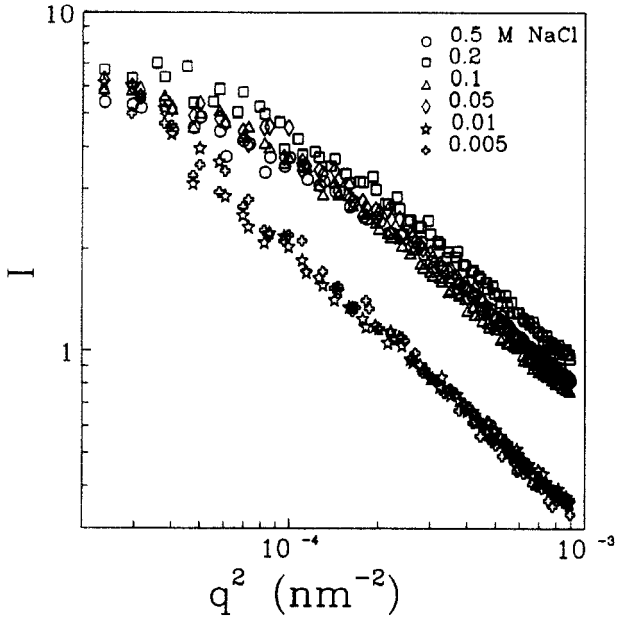

Figure 7. Scattering curves for solutions or supernatants with concentration C or initial concentration $C_i = 5.029 \times 10^{-5}$ g cm^{-3}, and with different salt contents. For 0.1, 0.2, and 0.5 M brine systems, there is no precipitate.

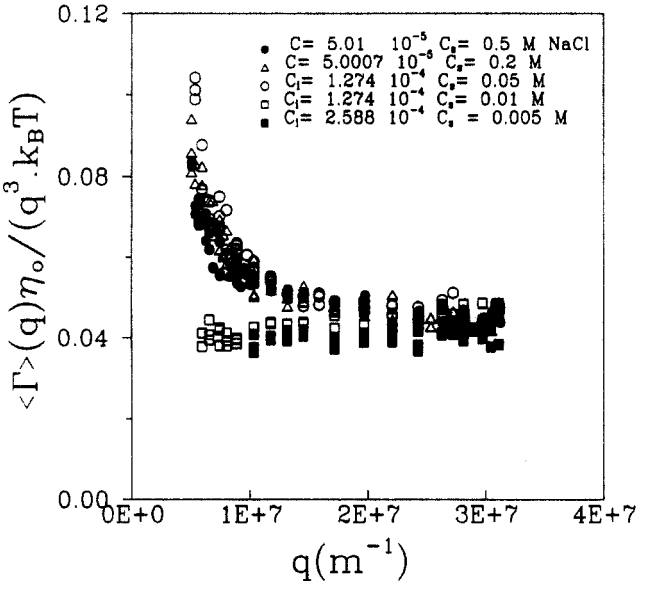

Figure 8. Dynamic scattering curves for solutions or supernatants at different polymer and salt concentrations; the concentration C refers to systems not having precipitated; the concentration C_i refers to the initial concentration, the measurements being made on the supernatants.

interactions. At a low salt content, attractive electrostatic interactions are dominant and the chains collapse. On the contrary, in the high salt limit, when the Debye–Hückel length becomes short enough that the Coulomb interactions are screened out, then the excluded volume interactions are dominant and the polymer has a swollen or Gaussian conformation, depending on the quality of the solvent.

The theoretical treatment of Higgs and Joanny predicts that the globule–coil transition of a neutral polyampholyte occurs when the salt concentration becomes larger than the concentration of polymeric charges within the globule.[16] Below the critical salt concentration, at finite polymer concentration, a phase separation is expected between a high concentration phase of interpenetrating Gaussian chains and a dilute solution in which each chain is a collapsed globule.

Table 1. Static Exponent α_s and Dynamic Exponent α_D Relative to the Scattering Measurements in the Intermediate Regime[a]

Part a

C_s (M)	C (g cm^{-3})	α_s	α_D	C_s (M)	C (g cm^{-3})	αs	α_D
0.5	2.3×10^{-5}	1.68		0.2	5.03×10^{-5}	1.66	2.8
"	5.01×10^{-5}	1.6	2.85	"	1.25×10^{-4}	1.64	
"	1.02×10^{-4}	1.6	2.8	"	2.5×10^{-4}	1.6	
"	5.09×10^{-4}	1.6	2.84	"	3.75×10^{-4}	1.6	
0.2	5×10^{-5}	1.68		"	5×10^{-4}	1.6	2.82

Part b

C_s (M)	C_i (g cm^{-3})	α_s	α_D	C_s (M)	C_i (g cm^{-3})	α_s	α_D
0.2[b]	1.62×10^{-5}	1.66		0.05	2.65×10^{-5}	1.55	
"	2.15×10^{-5}	1.66		"	5.02×10^{-5}	1.6	
"	1.29×10^{-4}	1.6		"	5.1×10^{-5}	1.63	2.85
"	2.59×10^{-4}	1.6		"	7.6×10^{-4}	1.5	2.98
0.1	2.5×10^{-4}	1.64	2.94	0.01	5.02×10^{-5}	1.66	
"	5.02×10^{-5}	1.6		"	1.27×10^{-4}	1.6	3.1
0.05	3.18×10^{-5}	1.65		0.005	1.62×10^{-5}	1.66	
"	5.02×10^{-5}	1.57		"	2.16×10^{-5}	1.66	
"	6.37×10^{-5}	1.64		"	5.02×10^{-5}	1.66	
"	1.25×10^{-4}	1.68	2.91	"	1.29×10^{-4}	1.58	
"	1.27×10^{-4}	1.6	2.89	"	2.59×10^{-4}	1.57	3.02

[a] $I(q) \propto q^{-\alpha_s}$. $(2\Gamma)^{-1} \propto q^{-\alpha_D}$; α_D was determined from the linear part of the log–log plots of $(2\Gamma)^{-1}$ versus q. The exponent α_s was obtained from the Fischer–Burford fit to the data for the solutions prepared in 0.5 and 0.2 M NaCl (Part a). For the supernatants obtained at lower salt content (Part b), α_s was determined from the linear part of the log–log representation of the scattering curves. In the later case, the concentration refers to the initial concentration C_i of the sample. [b] Precipitates obtained in 0.005 M NaCl, redissolved in 0.2 M NaCl.

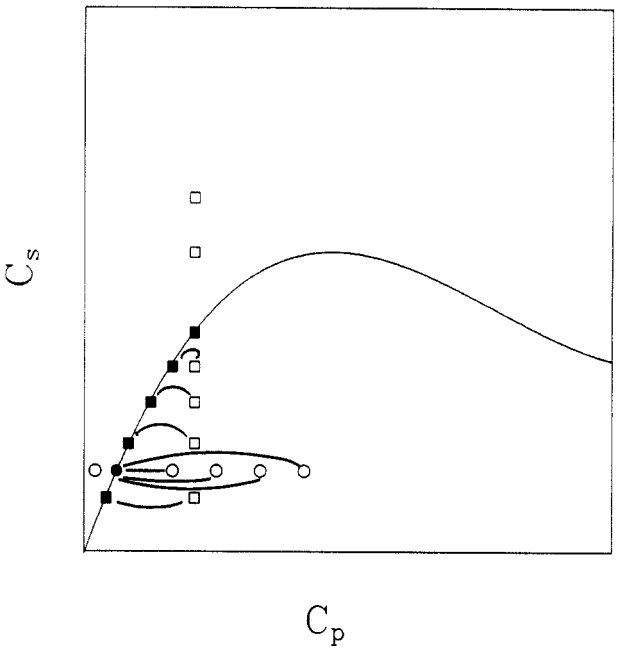

Figure 9. Schematic phase diagram for a polyampholyte with overall neutrality. Open squares represent systems with fixed polymer concentration and variable salt content. Below the solubility curves the systems undergo a phase separation, and the compositions of the supernatants are represented by the filled squares. Open circles represent systems with fixed salt concentration and variable polymer concentration. In that case, the supernatants of the diphasic systems have the same polymer concentration, represented by the filled circle.

Schematically, one can envision a phase diagram such as that shown in Figure 9. Upon decreasing the salt concentration C_s at a fixed polymer concentration C, one should observe, as one crosses the coexistence curve, a phase separation with a supernatant increasingly diluted. This is indeed observed experimentally, as inferred from the measurements of the intensity scattered from the

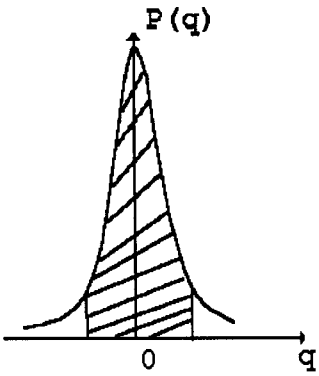

Figure 10. Schematic charge distribution of a polyampholyte. At low salt content, the chains with a low net charge (hatched part) precipitate whereas the chains with higher net charge (white area) remain in the supernatant.

supernatant that decreases steadily as the salt content is reduced (cf. Figure 7).

If now we keep C_s constant and increase C, we expect to observe a decrease of the volume of the supernatant, the polymer concentration in this phase remaining constant (cf. Figure 9).

The results are at variance with this prediction: the intensity scattered by the supernatant increases to the first order proportionally with the concentration of polymer dispersed prior to centrigugation (Figure 6). Also we would expect from the theory that the conformation of the macromolecules remaining in solution would be compact. In fact, the results of the table, relative to the exponent of $I(q)$ in the intermediate regime, indicate a swollen conformation of the chains.

To interpret the results obtained in this study, one must rather invoke a polydispersity of the net electrical charge carried out by the polyampholyte molecules. Such a polydispersity can be inferred from the variation of the copolymer composition with the degree of conversion[22,23] that shows that the incorporation of MADQUAT in the copolymer is faster than those of acrylamide or AMPS.[36] Therefore, we can assume that the sample consists of chains with a distribution of net charges of the kind schematically shown in Figure 10. In fact, we are dealing here with a situation similar to that described by Kantor et al.,[17] the origin of the charge distribution being however different. These authors consider the case where the constraint of charge neutrality assumed by Higgs and Joanny is released so that the polymers are randomly charged. Simulation and analytical arguments lead to the conclusion that the chains become stretched in pure water, due to a net charge imbalance. However, this effect should disappear for very high molecular weight polyampholytes.

In the presence of salt and for concentrations large enough to screen the electrostatic interactions, the polyampholyte behaves like a neutral polymer. The results relative to the asymptotic behavior of the scattered intensity suggest that the molecules adopt an excluded volume configuration. When the salt content is lowered, the neutral chains, i.e. those in the central part of the distribution, are expected to precipitate first, leaving chains with a finite net charge, i.e. the wings of the distribution, in the supernatant.

According to Higgs and Joanny,[16] the solubilization of neutral polyampholytes in a large excluded volume regime occurs at a salt concentration such that

$$\kappa^{-1} > \sim \frac{(fl)^{3/2}}{v^{1/2}b^{5/2}}$$

where f represents half the total number of charges, l is the Bjerrum length, v is the excluded volume parameter, and b is the length of the statistical unit. The theoretical model is not able to describe in detail the transition between collapsed and swollen molecules, but it is interesting to note that the authors speculate that the transition occurs without passing through the usual Θ point. This is what is effectively observed in this study, since the asymptotic exponent of the scattered intensity is always close to the excluded volume value.

Let us turn now to the case of the polymer chains with a net charge that are left in the supernatant.

The effect of salt on nonneutral polyampholytes has been considered by Joanny and Higgs.[16] The chain conformation results from the competition between the repulsive polyelectrolyte interactions and the attractive polyampholyte effect. The theory predicts that the nonneutral polyampholyte behaves in low salt solutions like a polyelectrolyte with a net charge. In particular, it is soluble in pure water. Upon increasing the salt content, the chain passes from linear to collapsed to swollen configuration. The salt content corresponding to the coil–globule transition depends on the net charge of the polymer.

In the present study, we observe that there is less and less polymer left in the supernatant as the salt concentration is lowered. Presumably, there are no or very few polymer chains soluble in pure water. This leads us to admit that the distribution of net charges is rather narrow and that the situation of neutral polyampholytes prevails. However, the higher the net charge, the lower the amount of salt required to screen the electrostatic interactions and therefore to solubilize the polyampholyte.

The experimental results also show that the chains solubilized in the supernatant of a low salt system are more swollen than those dissolved in high salt solutions. This surprising result suggests that, for polyampholytes with a small net charge, once suppressed the polyampholyte effect (screening of the interactions between charges of opposite signs), there is a persistence length left, may be due to the existence of small charged monomer blocks. In fact, the above observation is consistent with the Monte-Carlo simulations of Kantor et al.[17] that show that, due to charge fluctuations, the chains are stretched even in pure water, provided the system is dilute enough.

In this respect, it must be pointed out that the chains with opposite signs, present in the supernatant, are unlikely to form associated pairs in the dilute regime. On the other hand, in the semidilute regime the formation of such pairs might play a role in the precipitation of the polyampholytes. Even at high salt content, aggregates could form, thus giving rise to the slow mode observed in the autocorrelation function of the scattered intensity and to the anomalous behavior of the scattered intensity.

Figure 11 summarizes our observations relative to the phase diagram of the investigated systems. We have also tried to estimate the concentration of the supernatant obtained when a phase separation occurs. For doing so, we have compared the intensity scattered at 90° by the supernatant with the intensity scattered by the polymer with the same concentration under solvent conditions where it is entirely solubilized at high salt content (0.2 M). Of course, this method is very rough since we neglect the effect of interactions but it gives a general view of the behavior of the system upon variations of salt and polymer concentration. It must also be noted that the results relative to the phase separation are very reproducible.

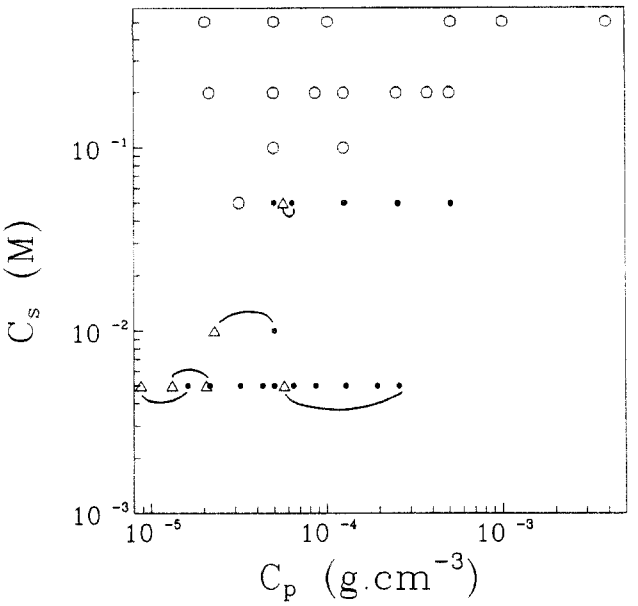

Figure 11. Actual phase diagram for the investigated sample. The open circles correspond to soluble samples, and the filled circles to samples for which a precipitate could be observed by eye; the triangles represent the concentrations of the supernatants estimated from the scattering intensities. The lines connect the initial systems to the corresponding supernatants.

Conclusion

The results reported in this study emphasize the influence of the distribution of charges along the chains of a globally neutral polyampholyte. This distribution strongly depends on the chemical synthesis method. The microemulsion polymerization leads to a monomer sequence distribution not far from random: due to different reactivity ratios of the monomers, the fluctuations of the net charge from chain to chain are larger than those that would be expected from a perfectly random distribution of charges.

At high salt content, the electrostatic interactions are screened out and all the chains are soluble. The chain conformation is that of the excluded volume regime. Below a critical salt content, the chains with a zero or small net charge precipitate, due to the polyampholyte effect. The supernatant contains highly swollen oppositely charged molecules. The polymer concentration in the supernatant decreases upon decreasing the salt content, the chains being more and more swollen. In other words, the phase separation observed here represents a fractionation process, not in terms of molecular weight distribution but rather in terms of a net charge distribution. Note that the mass polydispersity can also play a role since the collapse–swollen transition is very sensitive to the molecular weight of the polyampholyte.[16]

The next step of the study will be to compare the respective behaviors of polyampholytes prepared under different experimental conditions and therefore with different monomer sequence distributions.

Acknowledgment. The authors wish to thank J. F. Joanny, A. Johner, and F. Schosseler for helpful discussions. The financial assistance of the ELF-ATOCHEM group is gratefully acknowledged.

References and Notes

(1) Salamone, J. C.; Rice, W. C. In *Encyclopedia of Polymer Science and Engineering*, 2nd ed.; Mark, H. F., Bikales, N. M., Overberger, C. G., Menges, G., Eds.; Wiley: New York, 1987; Vol. 11, p 514.
(2) Bekturov, E. A.; Kudaibergenov, S. E.; Rafikov, S. R. *Rev. Macromol. Chem. Phys.* **1990**, *C30* (2), 233.
(3) Alfrey, T.; Morawetz, H.; Fitzgerald, E. B.; Fuoss, R. M. *J. Am. Chem. Soc.* **1950**, *72*, 1864.
(4) Katchalsky, A.; Miller, I. R. *J. Polym. Sci.* **1954**, *13*, 57.
(5) Hart, R.; Timmerman, P. *J. Polym. Sci.* **1958**, *28*, 638.
(6) Salamone, J. C.; Volsken, W.; Olson, A. P.; Israel, S. C. *Polymer* **1978**, *19*, 1157.
(7) Schulz, D. N.; Peiffer, D. G.; Argaval, P. K.; Larabere, J.; Kaladas, J. J.; Soni, L.; Handwerker, B.; Garner, R. T. *Polymer* **1986**, *27*, 1734.
(8) Peiffer, D. G.; Lundberg, R. D. *Polymer* **1985**, *26*, 1058.
(9) Monroy Soto, V. M.; Galin, J. C. *Polymer* **1984**, *25*, 254.
(10) Wielema, T. A.; Engberts, J. B. F. N. *Eur. Polym. J.* **1990**, *26* (6), 639.
(11) Salamone, J. C.; Watterson, A. C.; Hsu, T. D.; Tsai, C. C.; Mahmud, M. U. *J. Polym. Sci., Polym. Lett. Ed.* **1977**, *15*, 487.
(12) McCormick, C. L.; Johnson, C. B. *Macromolecules* **1988**, *21*, 686, 694.
(13) McCormick, C. L.; Salazar, L. C. *Macromolecules* **1992**, *25* (7), 1896.
(14) McCormick, C. L.; Salazar, L. C. *Polymer* **1992**, *33*, 4384.
(15) Edwards, S. F.; King, P. R.; Pincus, P. *Ferroelectrics* **1980** (GB), *30*, 3.
(16) Higgs, P. G.; Joanny, J. F. *J. Chem. Phys.* **1991**, *94* (2), 1543.
(17) Cantor, Y.; Li, H.; Kardar, M. *Phys. Rev. Lett.* **1992**, *69* (1), 61.
(18) Victor, J. M.; Imbert, J. B. *Europhys. Lett.* **1993**, *24*, 189.
(19) Higgs, P. G.; Orland, H. *J. Chem. Phys.* **1991**, *95* (6), 4506.
(20) Wittmer, J.; Johner, A.; Joanny, J. F. *Europhys. Lett.* **1993**, *24*, 263.
(21) Corpart, J. M.; Candau, F. *Colloid Polym. Sci.*, in press.
(22) Corpart, J. M.; Selb, J.; Candau, F. *Polymer* **1993**, *34*, 3873.
(23) Corpart, J. M.; Candau, F. *Macromolecules* **1993**, *26*, 1333.
(24) Koppel, D. E. *J. Chem. Phys.* **1972**, *57*, 4814.
(25) De Gennes, P. G. *Scaling concepts in polymer physics*; Cornell University Press: Ithaca, NY, 1979.
(26) Fisher, M.; Burford, R. *Phys. Rev. B* **1974**, *10*, 2818.
(27) Dietler, G.; Aubert, C.; Cannell, S. D.; Wiltzius, P. *Phys. Rev. Lett.* **1986**, *57*, 3117.
(28) Appell, J.; Porte, G. *Europhys. Lett.* **1990**, *12*, 185.
(29) Akcasu, A. Z.; Benmouna, M.; Han, C. C. *Polymer* **1980**, *21*, 866.
(30) Delsanti, M. Thesis, Université de Paris-Sud, 1978.
(31) Benmouna, M.; Akcasu, A. Z. *Macromolecules* **1978**, *11*, 1187.
(32) Akcasu, A. Z.; Han, C. C. *Macromolecules* **1981**, *14*, 1080.
(33) Lee, A.; Baldwin, P. R.; Oono, Y. *Phys. Rev. A.* **1984**, *30*, 968.
(34) Oono, Y. *J. Chem. Phys.* **1983**, *79*, 4629.
(35) Akcasu, A. Z.; Han, C. *Macromolecules* **1979**, *12*, 276.
(36) Neyret, S.; Selb, J.; Candau, F. To be published.